An analysis of the uneven tool electrode wear mechanism in the micro-electrical discharge machining process

Zhixiang Zou [1] · Xiaoyu Zhang [2] · Kangcheung Chan [3] · Taiman Yue [3] · Zhongning Guo [1] · Can Weng [2] · Jiangwen Liu [1,*]

1 State Key Laboratory of Precision Electronic Manufacturing Technology and Equipment, Guangdong University of Technology, Guangzhou 510006, PR China

2 State Key Laboratory of High Performance Complex Manufacturing, Central South University, Changsha 410083, PR China

3 Research Institute for Advanced Manufacturing, Department of Industrial and Systems Engineering, The Hong Kong Polytechnic University, Hung Hom, Hong Kong

*Corresponding author: Jiangwen Liu.

Tel: 86-20-39322412; Email: fejwliu@scut.edu.cn

Abstract

Micro-electrical discharge machining (micro-EDM) has an issue of uneven tool electrode wear that seriously affects the micro-hole accuracy. However, the mechanism of uneven tool electrode wear remains unclear. In this study, the uneven tool electrode wear mechanism has been studied both theoretically and experimentally. It was first discovered that the ultrafine debris particles produced by the EDM spark play a critical role in uneven tool electrode wear. A theoretical model was established to reveal the movement and distribution of debris by employing Einstein's tea leaf paradox i.e., classic

secondary flow theory and electrophoretic theory. According to this model, when the polarity is positive, the ultrafine debris aggregate gradually and adhere to the bottom of the micro-hole thereby forming a dynamic progressive parabolic profile debris layer. This dynamic debris layer shields the material to be removed by the micro-EDM. As a result, the tip of the tool electrode is unevenly worn into a conical concavity shape. Conversely, under negative polarity, the tip of the tool electrode is unevenly worn into a conical shape. A set of experiments was performed to verify the model and the results agreed well with the predicted values. Subsequently, a novel approach is propozed to eliminate the uneven tool electrode wear by alternating the positive and negative pulses. Using this method, uneven tool electrode wear can be avoided and high accuracy micro-holes without a complementary cone and/or conical concavity can be obtained.

Keywords Micro-EDM · Electrode wear · Ultrafine debris particles · Secondary flow theory · Machining accuracy

1 Introduction

Miniaturization is one of the most important trends in current manufacturing technology. There is a high demand for parts with micro-holes in many industries [1]. Hasan et al. [2] stated that typical micro-hole fabrication technologies include mechanical micro-drilling, laser machining, micro-electrochemical machining (micro-ECM), and micro-electrical discharge machining (micro-EDM). However, mechanical micro-drilling is limited by the strength and hardness of the workpiece material [3]. Nasrollahi et al. [4] reported that laser processing produces large machined hole tapers and limited depth-to-diameter ratios. In addition, the debris and burrs are also inevitable due to the ablation and melt expulsion coexist in laser machining process [5]. Electrochemical machining is

affected by the flow field, electric field, and chemical corrosion characteristics. As a result, the machining accuracy is difficult to control and there is inadequate repeatability [6]. In most applications, EDM is a non-contact machining method that allows the machining of nearly all conductive materials without limitations on the hardness and strength of the workpiece material [7]. Therefore, it has considerable advantages as a micro-machining process and is widely used to drill micro-holes in difficult-to-machine materials [8].

However, the tool electrode wear is an inevitable disadvantage of micro-EDM and is the main factor that affects machining accuracy [9]. In general, severe tool electrode wear occurs in the side and lengthwise directions during micro-EDM process [10]. During drilling, debris and bubbles are exhausted from the processing area through the sidewall gap. This results in abnormal discharges between the sidewall gap and the tool electrode, and eventually, the tool electrode wears along the lateral direction [11]. To address the issue of the micro-hole taper resulting from lateral wear, Ferraris et al. [12] proposed the use of sidewall-insulated tool electrodes to prevent the sidewall discharges from affecting the micro-hole taper during micro-EDM. Wang et al. [13] used electrodeposition to manufacture Cu-ZrB_2 composite-coated tool electrodes with better EDM electrical corrosion resistance compared to conventional electrodes. The shape accuracy of the micro-hole was improved when a Cu-ZrB_2 composite-coated tool electrode was used. Kumar et al. [14] machined a series of inclined holes on the surface of a cylindrical tool electrode and facilitated the exhaust of debris and bubbles through the inclined holes, thus reducing the sidewise wear. In addition, various micro-EDM machining parameters also have considerable influence on the sidewise tool electrode wear. D'Urso et al. [15] found that the discharge energy increased with the current, causing rapid sidewise wear and a larger taper at the tip of the electrode. For this reason, Jahan et al. [16] used an RC pulse power supply

to provide small discharge energies which reduced the sidewise wear. On the other hand, Yan et al. [17] reported that the anti-electrolysis power supply can provided the positive and negative voltage between the workpiece and the electrode, and hence, generate alternating discharge current so as to suppress electrode electrolytic corrosion and oxidization in the deionized water. Furthermore, Yang et al. [18] sated that the bipolar pulse machining can achieve larger material removal and efficient machining with limited tool wear than unipolar in the same condition. It is obvious that the energy of the pulse power supply and pulse type have an essential role in the tool electrode wear.

Lengthwise direction wear represents another mode of tool electrode wear. Lengthwise wear can result in the machining of blind holes in micro EDM drilling failing by not achieving the intended depth. Researchers have sought to eliminate the influence of lengthwise wear on the accuracy of the machining depth during micro-EDM drilling, as reported by Huan et al. [19]. Various attempts have been made to improve the depth accuracy of blind hole drilling with EDM. Mustafa et al. [20] used empirical models to compensate for lengthwise wear, but the randomness and complexity of the EDM process resulted in considerable discrepancies between the models and the experimental results. Therefore, Pei et al. [21] established an EDM electrode wear model based on electromagnetic theory. This model provides physical insight into the actual EDM situation and predicts the lengthwise wear more accurately than conventional geometric formulas. Jeong et al. [22] established a geometric simulation model of EDM tool electrode wear by considering the wear of the electrode end and corner. Aligiri et al. [23] proposed a new lengthwise wear compensation method based on the real-time estimation of micro-EDM material removal. While drilling 900 μm-deep micro-holes, the proposed method could decrease the error in depth to 4%. Malayath et al. [24] used a new compensation method to drill a series of holes of uniform depth using image processing techniques. The proposed method

89 limited the deviation to 0.3–1% of the intended hole depth.

90 However, in actual machining processes, the tool wear in the lengthwise direction varies at each
91 section of the tool electrode. With such uneven tool electrode wear, a concave surface is formed at the
92 center of the tool electrode tip, which results in the formation of a cone at the center of the micro-hole
93 bottom under specific drilling conditions [25]. In currently available systems, the axial feed cannot
94 compensate for the uneven tool electrode wear, thus, the formation of this uneven tool electrode wear is
95 a challenge to micro-hole accuracy. While Mitsui et al. [26] have observed this uneven tool electrode
96 wear, and such concavities at the center of the tool electrode tip were measured, further explanations
97 were not provided. Ekmekci et al. [27] stated that similar features were observed on the tool electrode
98 tips and micro-hole bottoms, especially when low pulse energy was used for micro-EDM. Two main
99 reasons have been attributed to the uneven tool electrode wear. The first one is related to variations
100 between the discharge intensities at the concerned edge and the tool electrode center, which were
101 analyzed as skin effects [28]. The skin effect phenomenon leads to a higher current intensity on the
102 external tool electrode surface while the probability of discharge is significantly higher at the bottom of
103 the micro-hole than at the center. Because of this, a cone forms at the micro-hole bottom, eventually
104 causing a conical concavity at the center of the tool electrode tip [29]. Another view is that a conical
105 concavity forms at the tip of the tool electrode during the micro-EDM drilling of micro-holes because
106 debris particles accumulate in a conical formation at the bottom of the micro-hole due to the formation
107 of the vortex and function as an electrode. As a result, electrical discharge material removal interaction
108 continues between these debris particles and the tool electrode. A cone is formed at the micro-hole
109 bottom and its complementary conical concavity shape emerges on the tip of the tool electrode [30].
110 However, it was found that the tip of the tool electrode is unevenly worn into a cone shape and its

complementary shape, i.e. conical concavity emerges at the micro-hole bottom when the polarity is negative. Obviously, this phenomenon cannot be explained by Ekmekci and Sayar's theory [30]. On the other hand, Ichikawa et al. [31] argued that during the micro-EDM process, carbon particles adhere to the anode surface and form a protective carbon layer, resulting in the uneven tool electrode wear. According to Ichikawa and Natsu's theory, more debris and carbon particles would be produced under larger pulse energy conditions. As a result, uneven electrode wear would be more serious when large pulse energy is used. However, just the opposite, it was found that the uneven tool electrode wear does not occur under large discharge energy condition [30]. Actually, this phenomenon also can not be explained by the skin effects theory. Obviously, the uneven tool electrode wear mechanism and its influence on the machining accuracy still require further study.

With the above background in mind, our work aims to study the uneven tool electrode wear mechanism in the micro-EDM process, and the ultrafine debris particles produced by the EDM spark have been found to play a critical role. A model has been established to study the movement and distribution of ultrafine debris particles based on the classic secondary flow theory and electrophoretic theory. According to this model, the shapes of the tool electrode and micro-holes can be predicted for various processing polarity conditions, and the study focuses on modeling the mechanism of the uneven tool electrode wear. Furthermore, a series of experimental studies are also used to verify the mechanism discussed above.

2 Theoretical analyses

2.1 Analysis of the debris particles

To further study the relationship between the debris particles and the uneven tool electrode wear,

133 debris particles were collected with different pulse energy (i.e. energy parameter 14, 101, 114, and 250).
134 Ekmekci et al. [30] previously measured the pulse energy, with the energy parameter increased from 14
135 to 250, the pulse energy increased from 0.66 μJ to 238.81 μJ. The experiments described herein were
136 performed using a micro-EDM machine (SX-200hpm, Sarix). In the present experiments, the
137 corresponding EDM parameters of these pulse energy parameters are shown in Table 1. Other
138 conditions were set at a voltage of 110 V, frequency of 250 kHz, and a spindle speed of 500 rpm. The
139 working medium was hydrocarbon oil, the workpiece 304 stainless steel, and the tool electrode was
140 made from tungsten carbide. Figure 1a shows SEM images of the debris particles produced by low
141 pulse energy, which are basically spherical in shape. Furthermore, Figure 1b shows the EDS spectrum
142 of the debris particles. The carbon, oxygen, iron, and tungsten contents were approximately 72.41 At%,
143 15.43 At%, 2.7 At%, and 9.47 At%, respectively, showing the main component in the debris is carbon
144 particles.

145 **Table 1** Details of pulse energy parameters

Energy parameter	Pulse voltage (V)	Pulse width (μs)	Peak current (A)
14	110	1.48	0.72
101	110	1.51	1.08
114	110	1.97	3.68
250	110	3	9.12

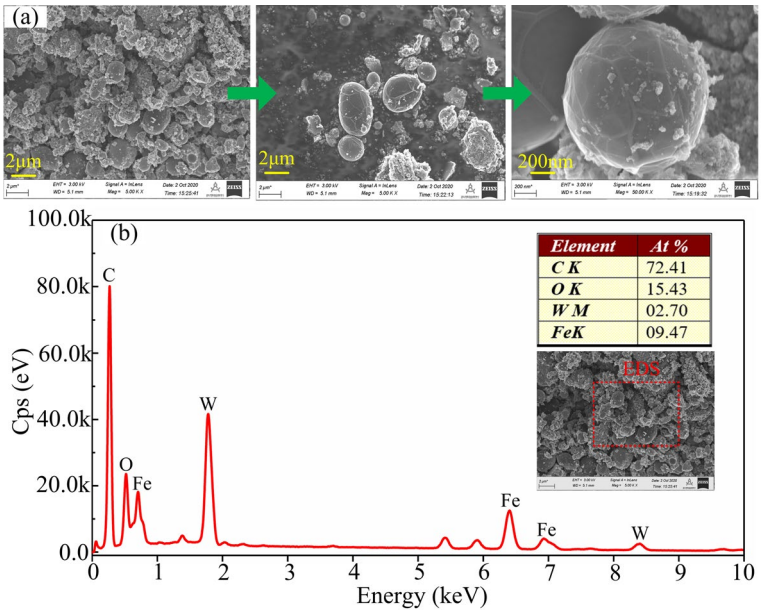

146

147 **Fig. 1 a** SEM images of the debris particles, **b** the EDS spectrum of the debris particles

148 A laser particle size analyzer (Litesizer 500) was used to measure the debris particle size
149 distribution produced by different pulse energy level. As can be seen from Fig. 2., the debris particle
150 size increases with the increasing of the pulse energy, while the uneven electrode wear decreases. This
151 result indicates that the uneven electrode wear is inversely proportional to the debris particles size,
152 which means that the smaller the particle size, the more obvious the uneven electrode wear
153 phenomenon. In the case of low pulse energy (energy parameter 14 and 101), most particles are smaller
154 than 1 μm (see Fig. 2a, b). These debris particles are classed as ultrafine debris particles in this study.
155 In contrast, most debris particles are larger than 1 μm under the large pulse energy conditions (energy
156 parameter 114 and 250) (see Fig. 2c, d). Large pulse energy means a high discharge energy. Thus, there
157 is no doubt that large pulse energy can produce larger debris particles. However, the experimental
158 results show that under large pulse energy conditions, uneven tool electrode wear cannot be observed
159 and micro-holes without a cone can be obtained (see Fig. 2d). Obviously, this phenomenon cannot be
160 explained by skin effects theory and/or carbon particles adhesion theory.

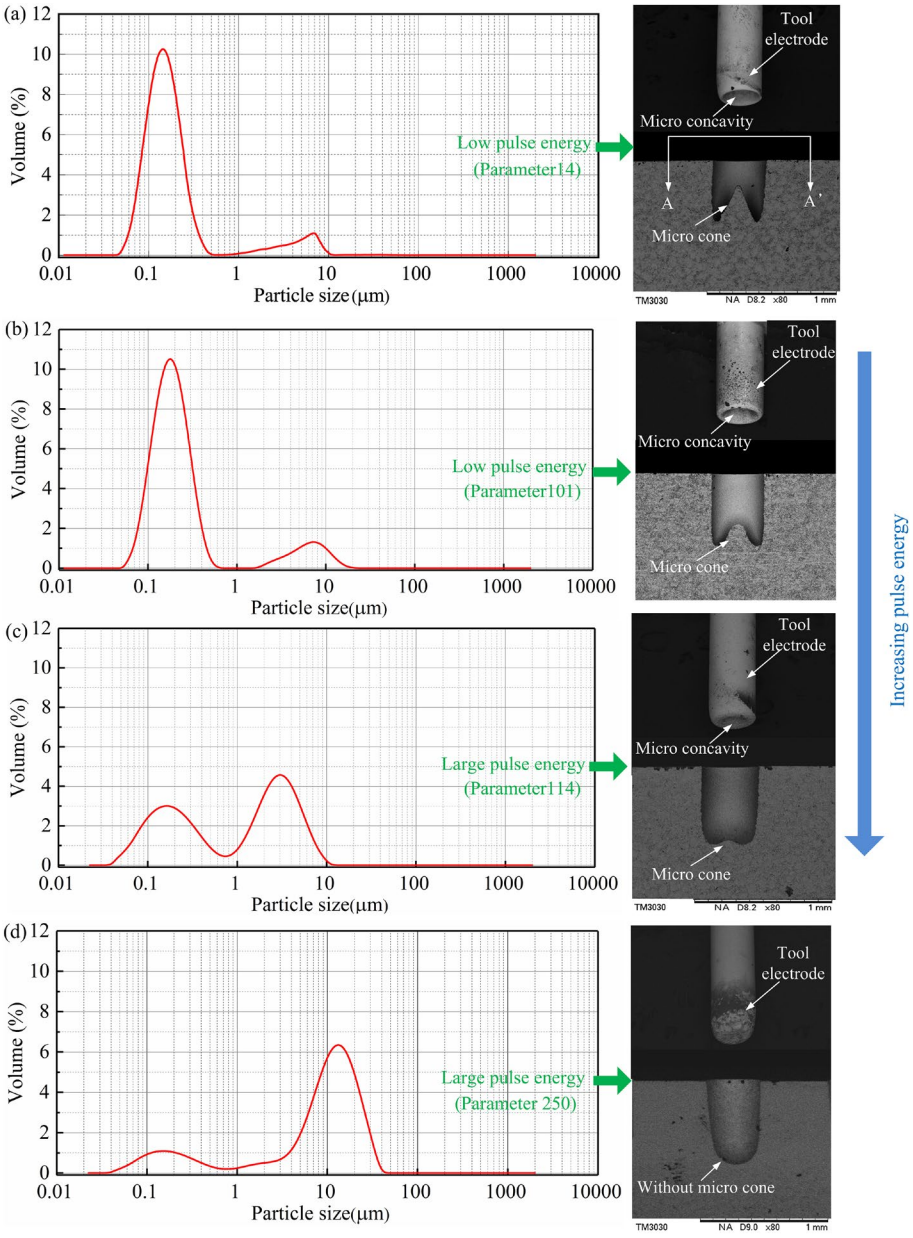

Fig. 2 Debris particle size distribution and tool electrode wear under different pulse energy condition: **a** parameter 14, **b** parameter 101, **c** parameter 114, and **d** parameter 250

2.2 Electrophoretic mobility of debris particles

Ikeno et al. [32] found that the ultrafine particles electrophoresise under the action of an electric field. The distance the particle travelled per unit time is called electrophoretic mobility. Large electrophoretic mobility indicates a strong electrophoretic effect [33]. Furthermore, the electrophoretic

mobility μ can be calculated by:

$$\mu = \frac{q}{6\pi\eta r} \quad (1)$$

where η is the solution viscosity, q is the charge, and the r is the particle radius. Clearly, Eq (1) shows that the electrophoretic mobility is inversely proportional to the radius of the debris particles, which means that the smaller the particle diameter, the higher the electrophoretic action. As shown in Fig. 2, the size of the debris particles generated at low pulse energy is much smaller than that under large pulse energy conditions, and therefore the electrophoretic effect of debris generated at low pulse energy is much stronger than that of large pulse energy. To further prove this assertion, a Zeta potential analyzer (Malvern, ZS90) was used to measure the electrophoretic mobility of debris particles. As shown in Fig. 3, with the increasing of the pulse energy, the electrophoretic mobility of the debris particles decreases. For instance, the electrophoretic mobility was -0.025 μmcm/Vs for low pulse energy (parameter 101). In comparison, the electrophoretic mobility was -0.0038 μmcm/Vs in the large pulse energy condition (parameter 250). Obviously, the debris particles generated at low pulse energy have a much stronger electrophoretic effect than those under large pulse energy conditions. On the other hand, the negative electrophoretic mobility of the particles indicates that the debris particles are negatively charged, and therefore the debris particles move towards the anode surface during processing.

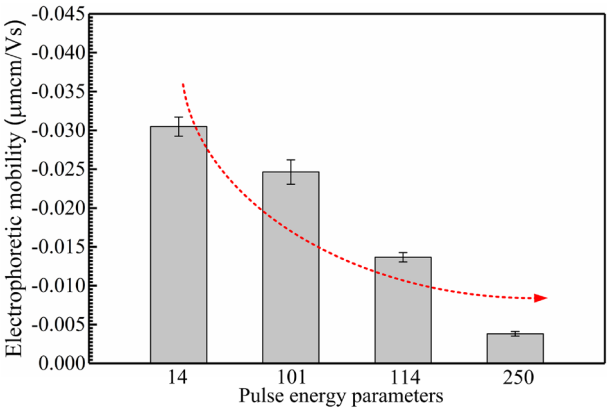

Fig. 3 Electrophoretic mobility of debris particles produced by different pulse energy

Thus, it is considered that the low pulse energy produces ultrafine debris particles with very high electrophoretic velocities. These ultrafine debris particles are quickly adsorbed on the anode surface during the process, thus causing uneven electrode wear. On the other hand, the electrophoretic velocity of the large particles produced under the larger pulse energy conditions is much smaller than that of the ultrafine particles, so the adsorption of large debris particles on the anode surface is not as pronounced as that for small particles. Thus, it is no surprise that the uneven tool electrode wear under high pulse energy conditions is not obvious. So, there is good a reason to believe that the strong electrophoretic effet of the ultrafine debris particles has a direct correlation with the uneven tool electrode wear.

2.3 Influence of the flow field on the tool electrode wear

To further explore the influence of the ultrafine debris particles on the uneven tool electrode wear, the micro-hole was drilled by a non-rotating tool electrode, and side flushing liquid was used to change the distribution of debris (see Fig. 4a). Other conditions were frequency, pulse voltage, spindle speed, and pulse energy of 250 kHz, 110 V, 0 rpm, and 101 (index), respectively. The tool electrode acts as the cathode, and the workpiece is the anode. As can be seen from Fig. 4b, c, when the tool electrode does not rotate, uneven tool electrode wear also exists. Interestingly, in this condition, the cone of the anode

surface is not in the center of the anode and shifts to the flushing liquid outlet side.

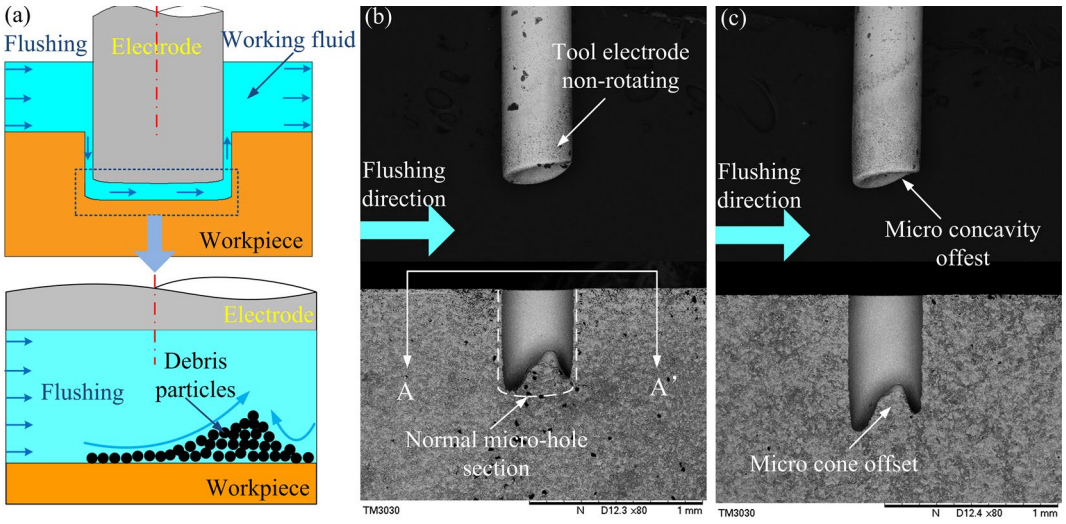

Fig. 4 a Schematic of the side flushing liquid without electrode non-rotating. Micro-hole and tool electrode tip after processing with different depths: **b** 600 μm, and **c** 800 μm

The shift of the cone to the liquid flushing direction may be caused by the accumulation of ultrafine debris particles at the outlet side. The experimental results further prove that the ultrafine debris particles are the main reason for the uneven tool electrode wear. There is good reason to believe that it is the synergistic effect of electric field and flow field that influence the distribution of the ultrafine debris particles, and thus influence the tool electrode wear process.

2.4 Classic secondary flow theory – Einstein's tea paradox

In the actual micro-EDM drilling process, the electrode is usually rotating. Therefore, the flow field and debris distribution under the electrode rotation condition was studied in detail. As noted, there are many typical secondary flow phenomena related to fluid flow that contain particles, such as the river bending phenomenon shown in Fig. 5. In 1926, Einstein [34] discussed the reason for river bending. Another interesting phenomenon, also noted in his investigation, was when chopsticks were used to stir tea in a cup, it is intuitively expected that the tea leaves move to the bottom edge of the cup

due to the centrifugal force. Contrary to expectation, the tea leaves gather at the center of the bottom of the cup; the famous Einstein's tea leaf paradox i.e. classic secondary flow theory (see Fig. 6). As for micro-EDM, the rotation of the tool electrode causes the working liquid in the inter-electrode gap to rotate and the distribution of the debris particles in the working fluid resembles that of tea leaves in a cup. Therefore, in the next section, the distribution of ultrafine debris particles is analyzed based on the classic secondary flow theory and electrophoretic theory.

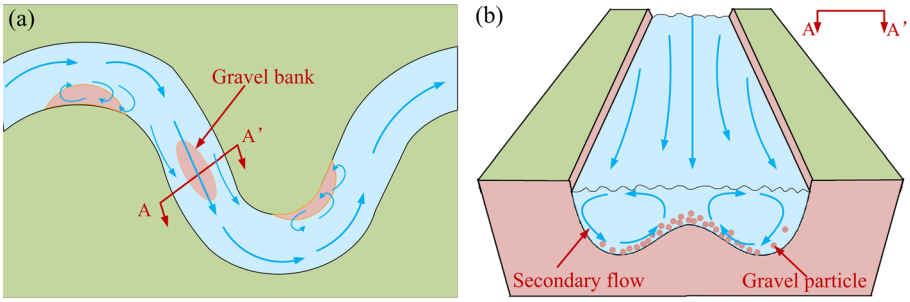

Fig. 5 a The river bending phenomenon, and **b** secondary flow effect

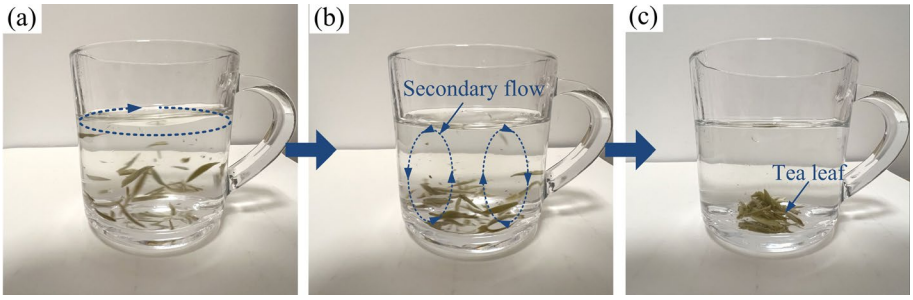

Fig. 6 Distribution of the tea leaf: **a** stirring the tea, **b** generation of secondary flow, and **c** tea leaf gathered at the center of the cup bottom

2.5 Theoretical model for ultrafine debris particles distribution

To investigate the flow field distribution of the inter-electrode gap, a model was established using COMSOL Multiphysics software. Figure. 7a shows the three-dimensional (3D) geometrical model developed for the EDM drilling of micro-holes. The model is symmetrical in the X direction and the geometry can be simplified into a two-dimensional (2D) model, as shown in Fig. 7b. In this simulation,

the working fluid is kerosene. The following assumptions are made to simplify the model: (1) the fluid is continuous and incompressible, (2) there is no bubbles generation, and (3) material removal is not considered. The simulation conditions are listed in Table 2.

The fluid model is governed by the Navier–Stokes equations, and the standard turbulence model was used to solve the flow field:

$$\rho\frac{\partial u}{\partial t}+\rho(u\cdot\nabla)u=\nabla\left[-pI+\mu\left(\nabla u+(\nabla u)^{T}\right)\right]+F \tag{2}$$

$$\nabla u=0 \tag{3}$$

where u is the velocity (m/s), ρ is the density (kg/m^3), μ is the dynamic viscosity (Pa·s), p is the pressure (Pa), T is the absolute temperature (K), F is the volumetric force (N), and I is the identity matrix.

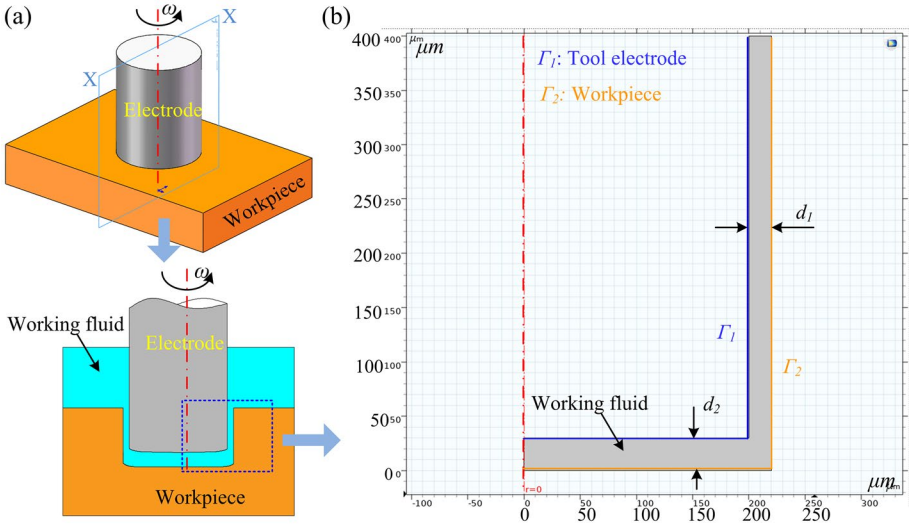

Fig. 7 Simulation model for flow field distribution: **a** three-dimensional model, **b** two-dimensional geometrical models

Table 2 Parameters for flow field simulation

Item	Value	Unit
Tool electrode diameter	400	μm
Spindle speed	500	rpm
Depth of micro-hole	400	μm
Side gap /d_1	20	μm
Machining gap /d_2	30	μm

The flow field under the rotational tool electrode is shown in Fig. 8. The arrows in the streamlines are arranged equally, and the streamline contour reveals the distribution of the flow field. As can be seen, the flow velocity gradually decreases from the outer edge to the center of the axis of symmetry. Clearly, there is a typical secondary flow phenomenon in the inter-electrode gap. However, it should be noted that the working liquid contains numerous debris particles, so the electrophoretic adsorption characteristics of ultrafine debris particles need to be considered.

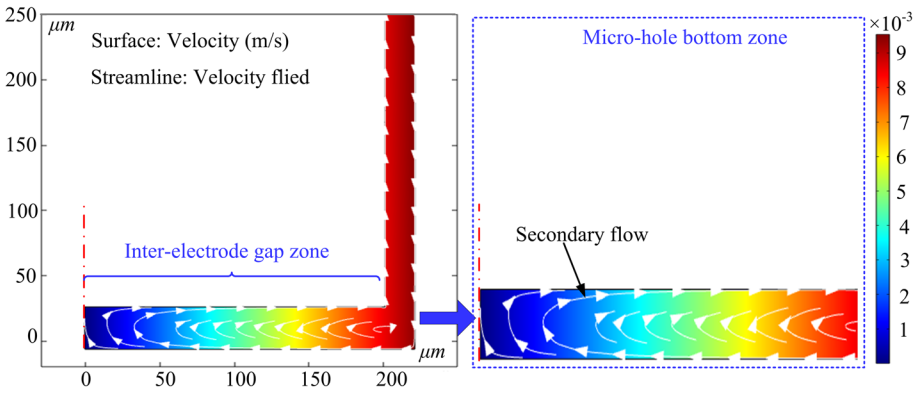

Fig. 8 The results of flow field distribution with the tool electrode rotating

As discussed earlier, the movement and distribution of the ultrafine debris particles are influenced by the combined effect of the flow and electric fields. Obviously, the distribution of ultrafine debris particles is infulenced by electrophoretic effect. For instance, when the polarity is positive, some debris particles move to the center of the axis under the action of the secondary flow effect. Owing to the electrophoretic effect, the ultrafine debris particles aggregate and adhere to form a progressive

parabolic profile debris layer at the bottom of the micro-holes, as shown in Fig. 9a. In contrast, when a negative polarity is used, the tool electrode is the anode, and the ultrafine debris particles are subjected to an upward electrophoretic force. Under the action of the secondary flow and the electrophoretic effect, the particles continue to rise and adhere to the center of the tool electrode tip. This leads to the formation of a progressive parabolic profile debris layer on the tip of the tool electrode, as shown in Fig. 9b.

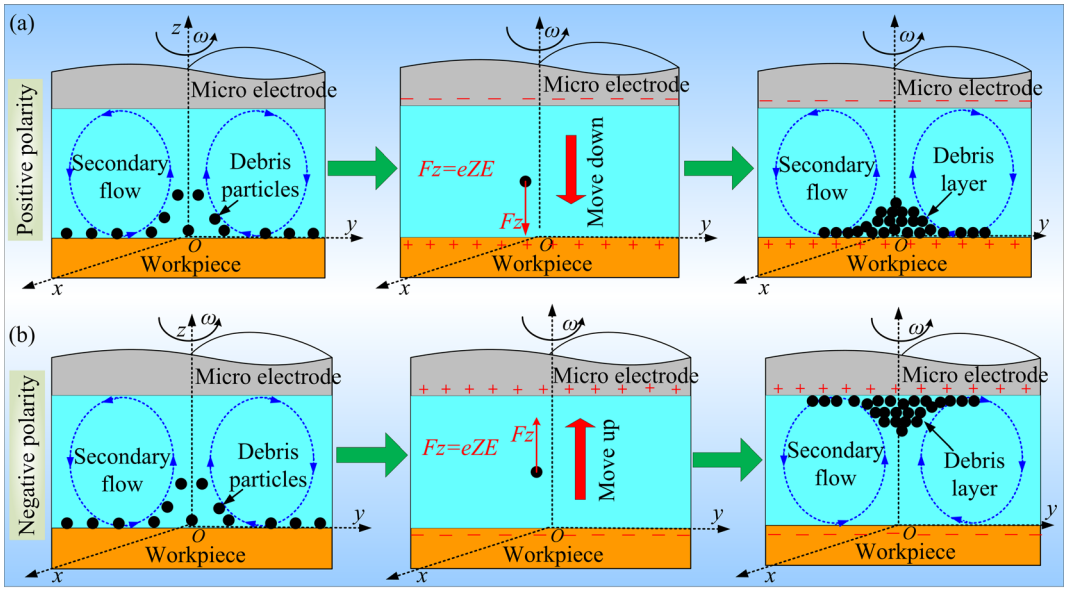

Fig. 9 Schematic of ultrafine debris particles distribution under different polarities: **a** positive polarity, and **b** negative polarity

Moreover, it should be noted that the thickness of the debris layer is unevenly distributed due to the secondary flow effect. The thickness of the progressive parabolic profile debris layer in the central region is large but the edges are thin. Accordingly, the electric field strength increases gradually from the edge to the center. It is well known that a higher electric field strength area provides a greater amount of electrical discharge than that of other areas. Although the electrical discharge takes place at the debris layer, a progressive parabolic profile debris layer is produced dynamically and has a

shielding effect. Eventually, this debris layer leads to uneven material removal, such as the speed of material removal being slow in the center and fast at the edges.

When positive polarity is used, a dynamic debris layer forms at the bottom of the micro-hole, that leads to a decrease in the material removal speed from the edge to the center of the micro-hole during the micro-EDM process. As a result, the bottom of the micro-hole continues to exhibit non-uniform removal, and a cone forms at the bottom of the micro-hole. Similarly, the tip of the tool electrode is unevenly worn into a corresponding conical concavity, as shown in Fig. 10.

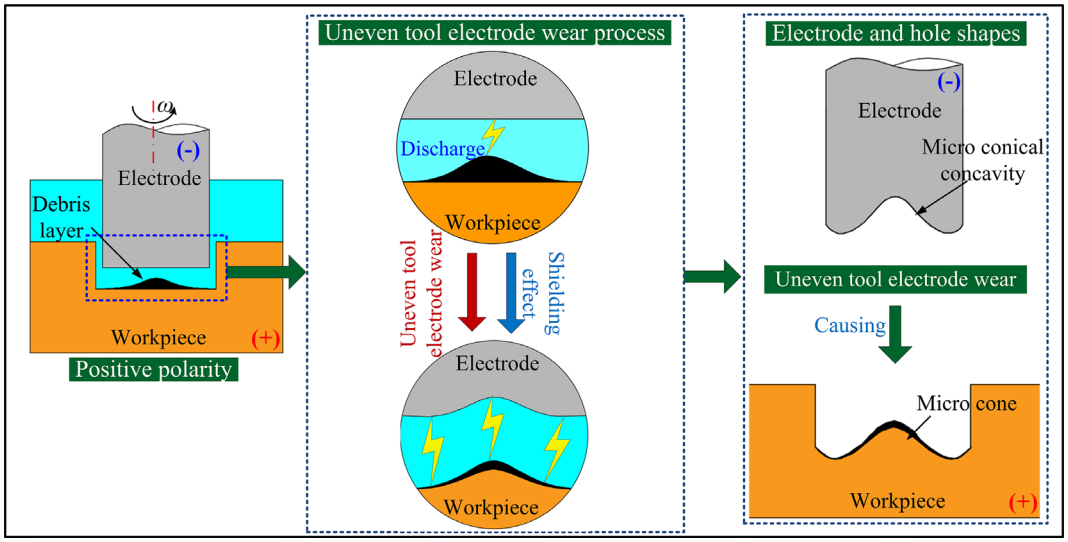

Fig. 10 Schematic of the effects of positive polarity on the machining

In contrast, when the polarity is negative, the debris particles aggregate and adhere at the tip of the tool electrode to form a dynamic progressive parabolic profile debris layer. The tool electrode tip has a shielding effect owing to the debris layer. Specifically, the material removal speed decreases from the edge to the center of the tool electrode tip. Thus, the tool electrode tip is unevenly worn into a cone shape, and a conical concavity is formed at the micro-hole bottom, as shown in Fig. 11.

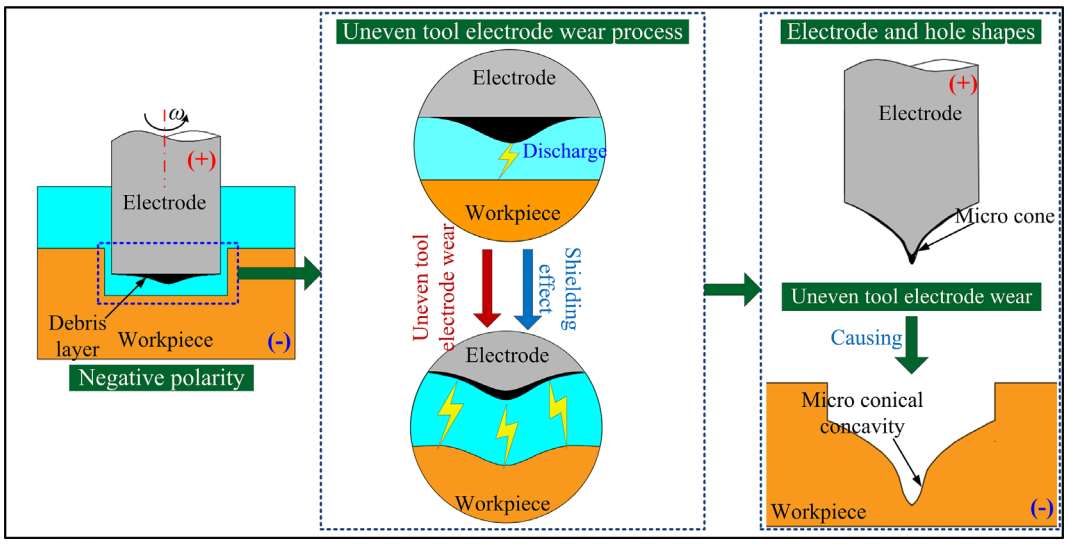

Fig. 11 Schematic of the effects of negative polarity on the machining

Using this model, the shapes of the tool electrode tips and micro-holes can be predicted under various polarity conditions. It can be speculated that the secondary flow movement and electrophoretic characteristics of the ultrafine debris particles are the main reasons for uneven tool electrode wear. For verifying the model, the uneven tool electrode wear mechanism was further studied experimentally.

3 Experimental procedures

3.1 Experimental setup

All the experiments described herein were performed using a micro-EDM machine (SX-200hpm, Sarix). The maximum ranges for machine table travel were 200 mm in the X direction, 100 mm in the Y direction, and 300 mm in the Z direction, with a step resolution of 1 μm. The spindle rotation speed could be adjusted between 0 and 500 rpm.

3.2 Materials and methods

The workpiece was made of stainless steel SUS304 and had dimensions 60 × 30 × 2 mm. A tungsten carbide (WC) rod with a diameter of 400 μm was selected as the tool electrode. Hydrocarbon

316 oil was used as the working fluid, and, the workpiece was fixed on an XY stage, and the tool electrode
317 was clamped on the spindle. After each micro-hole was drilled, the tip of the tool electrode was cut to
318 ensure that the electrode tip was flat when drilling of the next hole began. Details of the experimental
319 conditions are given in Table 3.

320 **Table 3** Processing conditions for the experiment

Item	Value
Frequency	250 kHz
Voltage	110 V
Energy parameter	101 (index)
Machining depth	200, 600, and 800 μm

321 Before and after micro-EDM machining, the workpiece and the tool electrode were cleaned with
322 ethanol solution for 3 min. After cleaning, the samples were dried and then tested. Moreover, to
323 observe the cross-section topography, micro-holes were cut along the horizontal section using a
324 low-speed wire cutting EDM machine. To analyze the debris layer, the samples were polished.
325 Microstructural analysis and observations were carried out on a scanning electron microscope (SEM)
326 using energy-dispersive X-ray spectroscopy (EDS). The tip of the tool electrode was also observed
327 likewise.

328

329 **4 Experiment verification of the theoretical model**

330 **4.1 Effect of positive polarity on the micro-hole and tip of tool electrode**

331 Micro-holes were drilled using frequency, pulse voltage, spindle speed, and low pulse energy of
332 250 kHz, 110 V, 500 rpm, 101 (index), respectively. The tool electrode was set up as the cathode, and
333 the workpiece selected as the anode. Figure. 12 shows the images of the tool electrode tips and

sectional views of micro-holes. As can be seen, there is an apparent cone at the center of the micro-hole bottom. Moreover, the tool electrode tips show a close approximation to the complementary shape of the micro-hole geometry. These changes are consistent with the results noted by Ekmekci et al. [30].

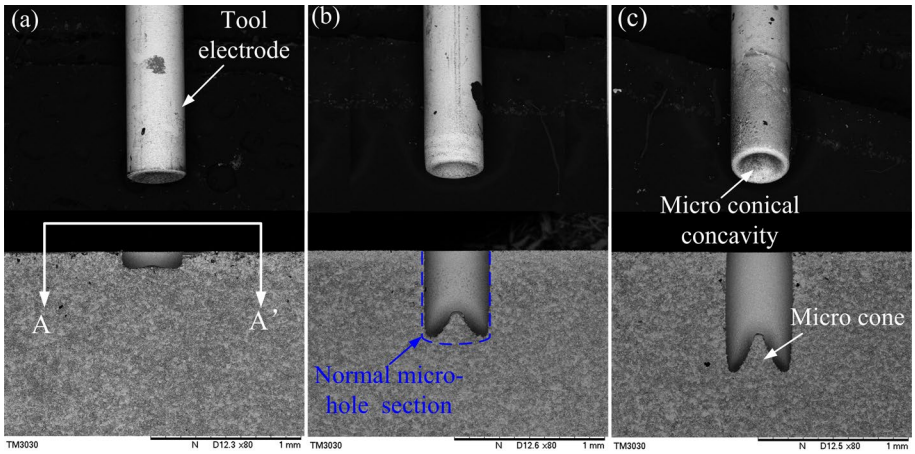

Fig. 12 Micro-hole and tool electrode tip after machining using a positive polarity processing with different machining depths: **a** 200 μm, **b** 600 μm, and **c** 800 μm

According to the theoretical model, this effect may be ascribed to the secondary flow movement and electrophoretic characteristics of the ultrafine debris particles. It is envisaged, when the polarity is positive, a dynamic progressive parabolic profile debris layer forms at the bottom of the micro-hole in the ignition delay stage and has a shielding effect in the spark discharge phase (see Figs. 10 and 13). As noted, the debris layer thickness in the central region is large but the edges are thin due to the secondary flow effect. Since electrical discharge material removal interactions between this debris layer and the tool electrode continue, non-uniform material removal occurs both in the workpiece and at the tip of the tool electrode. At the bottom of the micro-hole, the material removal speed decreases from the edge of the micro-hole to the center, and thus the center of the micro-hole bottom presents a cone formation. Similarly, the tool electrode undergoes more wear in the central region while little material is removed from the edges of the tool electrode tip. Therefore, the tool electrode tip is unevenly worn into a conical concavity. In particular, some carbon particles with high melting point might be welded

onto the anode surface due to the thermal effect of the spark (see Fig. 13b).

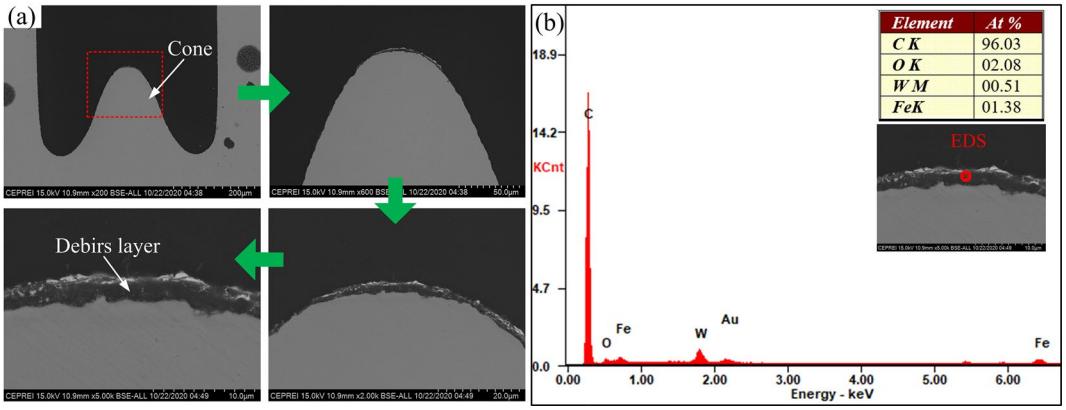

Fig. 13 a Sectional views of micro-holes, and **b** EDS spectrum of the debris layer with low pulse energy

To determine whether the thickness distribution of the debris layer agrees with the results of the theoretical model, the debris layer thickness was measured. The debris layer thickness was distributed unevenly as shown in Fig. 14a. More specifically, the thickness at the center of the cone was approximately 3 μm, the lateral edge approximately 1 μm, and the bottom less than 1 μm, as shown in Fig. 14b. That is to say, the debris layer thickness increased gradually from the edge of the cone to the center. Obviously, the thickness distribution of the debris layer is consistent with the model results.

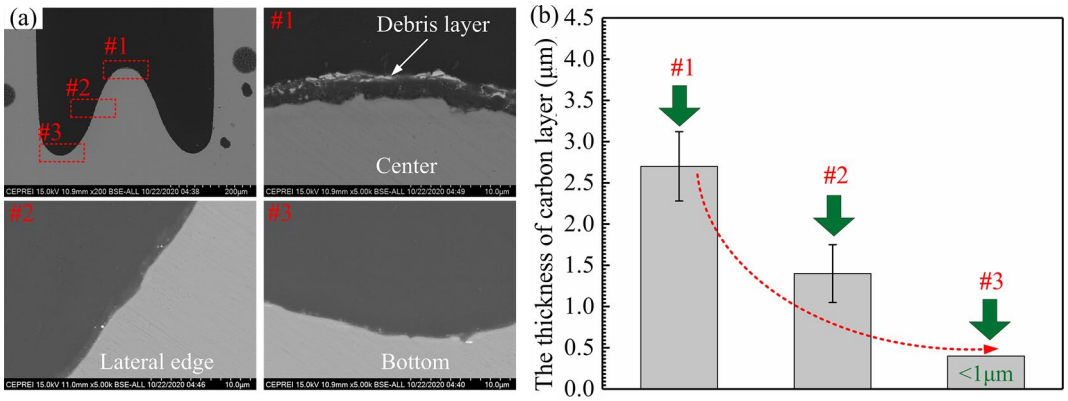

Fig. 14 a Sectional SEM images of the cone debris layer, and **b** the thickness of the debris layer

366 **4.2 Effect of negative polarity on micro-hole and tip of the tool electrode**

367 In a negative polarity machine, the micro-hole drilling conditions are frequency, pulse voltage,
368 and spindle speed of 250 kHz, 110 V, and 500 rpm, respectively. The tool electrode acts as the anode,
369 and the workpiece is the cathode. Figure. 15 shows the images of the tool electrode tips and sectional
370 views of the micro-holes. There is a significant uneven tool electrode wear phenomenon, and the tool
371 electrode tip is unevenly worn into a cone shape. Accordingly, the micro-hole bottom presents a conical
372 concavity. As indicated in the model, the ultrafine debris particles gradually aggregate and adhere to the
373 tool electrode tip to form a debris layer under negative polarity conditions. However, the debris layer is
374 thickest at the center of the tool electrode tip and thins gradually towards the outside. The tool electrode
375 tip has a shielding effect that leads to non-uniform electrode material removal. Specifically, the
376 material removal speed decreases from the edge of the tool electrode tip to the center, resulting in
377 uneven tool electrode wear (see Fig. 15). The tool electrode tip is unevenly worn into a cone shape,
378 while a conical concavity is formed at the micro-hole bottom. In the case of negative polarity as well,
379 the experimental results are consistent with the model results.

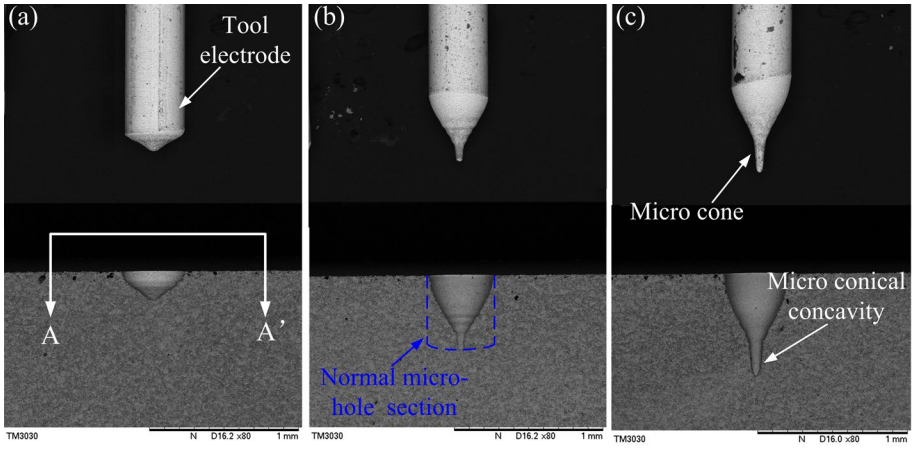

380

381 **Fig. 15** Micro-hole and tool electrode tip after processing using a negative polarity processing with
382 different machining depths: **a** 200 μm, **b** 600 μm, and **c** 800 μm

383 To further verify that the debris layer adheres to the tool electrode tip and causes the uneven

electrode wear under the negative polarity condition, the tool electrode tip was analyzed using the EDS spectrum. Figure. 16 shows the EDS spectrum of the tool electrode tip. As can be seen, from the center of the tool electrode tip to the lower edge, the atomic fraction of debris (C) decreases from 95.39 At% to 75.53 At%. This indicates that the debris particles distribution decreases from the center of the tool electrode tip to the edge and is consistent with the debris particle distribution laws predicted by the model results. Therefore, it can be concluded that there are secondary flow and electrophoretic adsorption effects in the micro-EDM process.

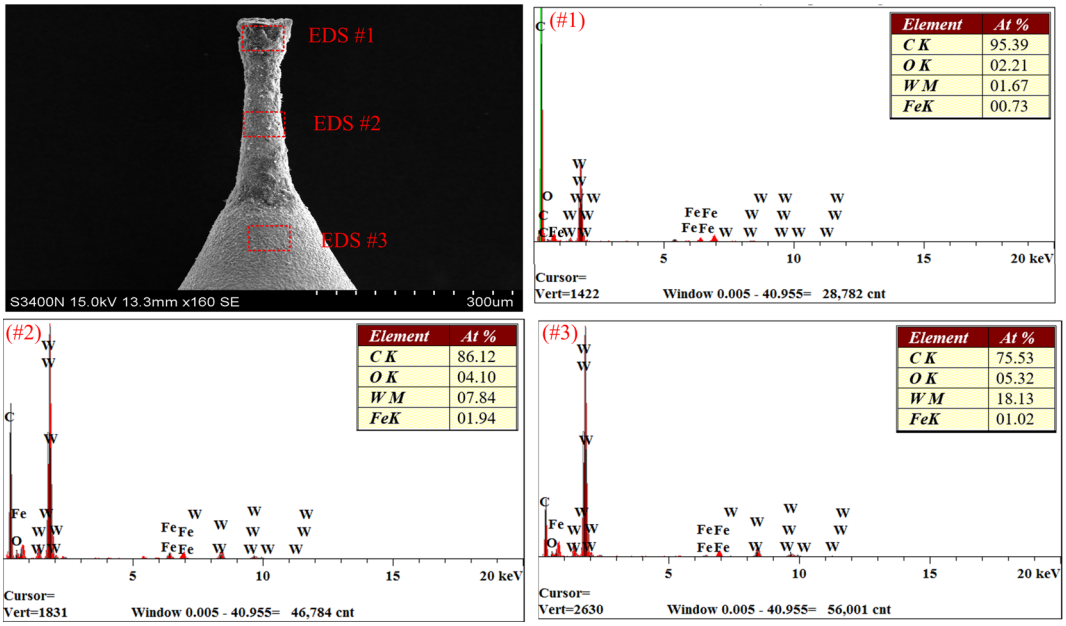

Fig. 16 EDS spectrum of the tool electrode after negative polarity processing

These experimental results indicate that the ultrafine debris particle effect is the main reason for uneven tool electrode wear. As discussed in section 2.1, debris particles produced by large pulse energy are much larger than those of low pulse energy (see Fig. 2). Theoretically, these large debris particles also aggregate and form a debris layer on the anode surface under the effect of the secondary flow and electrophoretic. However, on the one hand, compared to ultrafine debris particles the electrophoretic velocity of the large particles might be too low to form a stable protective layer on the anode surface

399 under very small pulse width conditions. On the other hand, large pulse energy provides a high
400 discharge energy, which leads to a decrease in the shielding effect of the debris layer. Thus, the uneven
401 tool electrode wear is not obvious under the large pulse energy condition.
402
403 **5 Elimination of uneven tool electrode wear**
404 Though micro-holes without cones and/or conical concavities can be fabricated by applying a
405 large pulse energy, such energy cannot be used to machine extremely small structures. With the
406 increasing miniaturization of parts, smaller and smaller discharge energy need to be used in the
407 micro-EDM process [16]. However, in the small discharge energy condition, uneven tool electrode
408 wear is an unavoidable issue that seriously affects the micro-hole accuracy. Recognising these
409 problems, it is apparent that the uneven tool electrode wear problem must be further improved in order
410 to meet the challenge in facing machining extremely small structures. As discussed earlier, the ultrafine
411 debris particles produced by small discharge energy are primary reason of uneven tool electrode wear.
412 Additionally, the adsorption direction of the ultrafine debris particles changes with the change of
413 polarity.
414 Based on the theoretical model and experimental results, a novel approach was developed to
415 eliminate the uneven tool electrode wear by alternating the positive and negative pulses. Figure. 17
416 illustrates the principle of this approach; in the case of positive polarity, the ultrafine debris particles
417 aggregate and adhere at the center of the micro-hole bottom and form a debris layer. This results in the
418 tool electrode tip being unevenly worn into a conical concavity (see Fig. 17b). In contrast, when using
419 negative polarity, the ultrafine debris particles fill the conical concavity on the tool electrode tip. That
420 is to say, the ultrafine debris particles can compensate for uneven tool electrode wear via the secondary

flow and electrophoretic effects. Thus, electrical discharge continues between these debris layers and the micro-hole cone (see Fig. 17c). By setting the positive and negative pulse machining ratio to compensate for uneven tool electrode wear, can eliminate the cone of micro-hole bottom (see Fig. 17d).

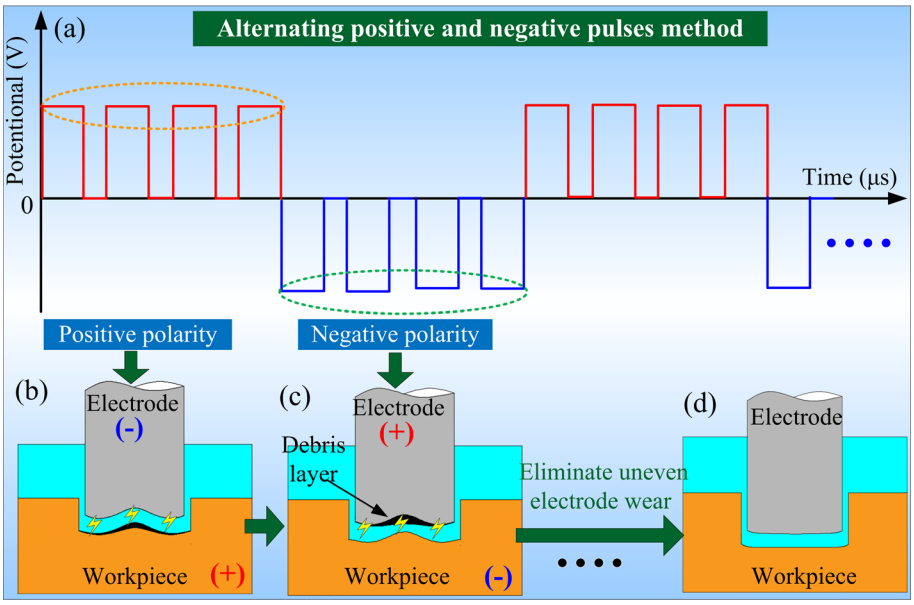

Fig. 17 Schematic of alternating positive and negative pulses method

In this experiment, the frequency, voltage, pulse energy, and spindle speed were set to 250 kHz, 110 V, 101 (index), and 500 rpm, respectively. In addition, the ratio of positive-to negative-polarity machining was determined based on the electrode feed parameters. the ratio of positive to negative polarity was set at 1:0, 3:1, 3:2, 1:1 and 0:1, respectively. As shown in Fig. 18a, when ratio of positive to negative polarity is 1: 0 i.e., under the positive polarity condition, a cone forms at the bottom of the micro-hole and the tip of the tool electrode is unevenly worn into a corresponding conical concavity. It was found that the height of the cone i.e., uneven tool electrode wear decreases with the increasing of the negative polarity ratio (see Fig. 18b, c). And a flatter micro-hole bottom can be obtained under 3:2 positive to negative polarity ratio condition, which means that uneven tool electrode wear can be avoided as shown in Fig. 18c. Moreover, as the proportion of negative polarity continues increases, the center of the micro-hole bottom appears a conical concavity gradually, whereas the tool electrode tips

is unevenly worn into a micro cone shape (see Fig. 18d, c). Clearly, the uneven tool electrode wear can be easily avoided and high accuracy micro-holes without the cone and/or conical concavity can be obtained under proper positive to negative polarity ratio.

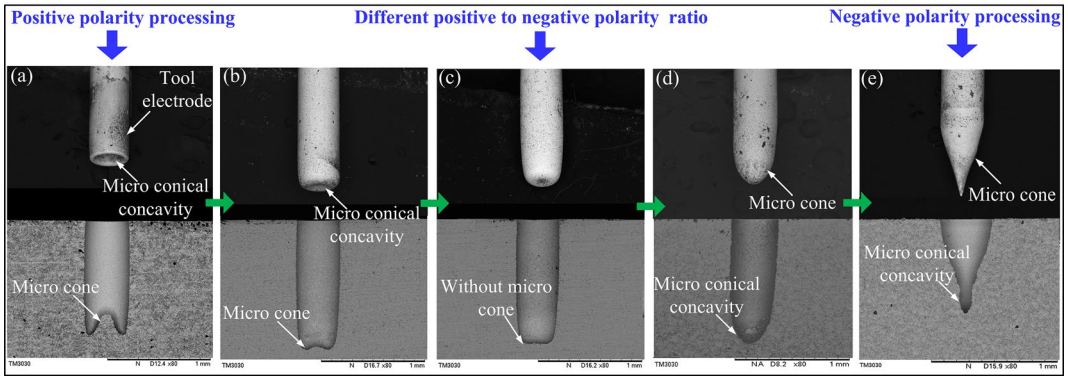

Fig. 18 SEM images of electrode tool tip and section of the micro-holes under different positive to negative polarity ratio: **a** 1:0, **b** 3:1, **c** 3:2, **d** 1:1, and **e** 0:1

The micro-holes machined under 3:2 positive to negative polarity ratio were analyzed by SEM and EDS. Figure. 19a shows the SEM images of enlarged sectional views of the micro-holes bottom. Both the SEM image and the EDS spectrum (see Fig. 19b) of the micro-hole bottom show that there is almost no debris layer adhered onto the micro-hole bottom. These findings demonstrate the potential of alternating positive and negative pulses method. It with reason to believe that the uneven tool electrode wear can be eliminated in the micro-EDM process by using this novel method.

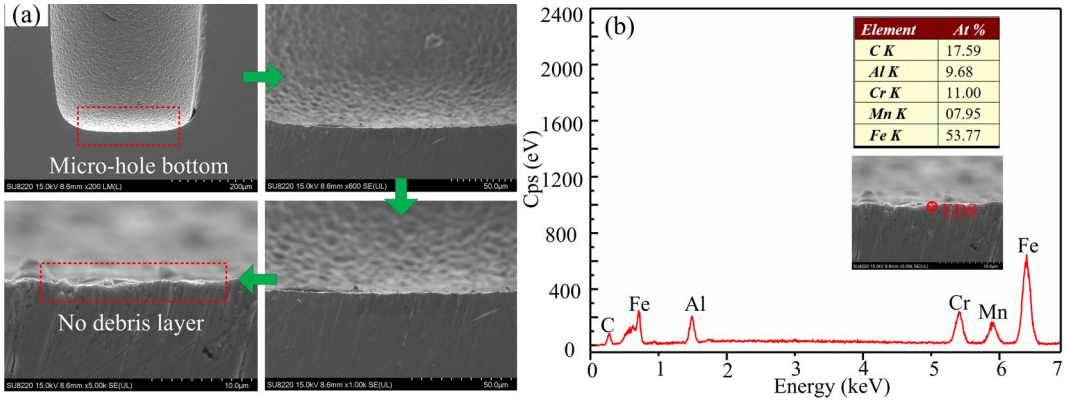

Fig. 19 a Sectional views of micro-holes, and **b** EDS spectrum of the debris layer with alternating positive and negative pulses method

6 Conclusions

This study used the secondary flow theory and electrophoretic theory to investigate the uneven tool electrode wear mechanism during micro-EDM process. It was found that ultrafine debris particles produced by the EDM spark play a critical role in the uneven tool electrode wear. A theoretical model was established to reveal the movement and distribution of the ultrafine debris particles. Based on the theoretical model, a new method is proposed to eliminate the uneven tool electrode wear. The critical conclusions of this study are summarized as follows:

(1) It was found that ultrafine debris particles are produced during the micro-EDM process. These ultrafine debris particles adhere onto the anode electrode surface due to the electrophoretic effect.

(2) A theoretical model was established to study the ultrafine debris particles movement and distribution in the micro-EDM area. The simulation results showed that under the effect of the secondary flow and electrophoretic, the ultrafine debris particles aggregate and form a progressive parabolic profile dynamic debris layer on the anode surface.

(3) The dynamic debris layer shields the anode materials from removal by the micro-EDM spark. The dynamic progressive parabolic profile debris layer thickness increases gradually from the anode edge to the center. Accordingly, the material removal speed increases from the anode edge to the center. Thus, in the case of positive polarity, a cone is formed at the micro-hole bottom, eventually causing a conical concavity at the center of the tool electrode tip. Conversely, under the negative polarity condition, the tool electrode is unevenly worn into a cone shape, and its complementary shape, i.e. conical concavity emerges at the micro-hole bottom.

(4) Based on the developed theoretical model, a novel approach is proposed to eliminate uneven tool electrode wear. By alternating the positive and negative pulses, uneven tool electrode wear can be

avoided and high accuracy micro-holes without cone and/or conical concavity can be obtained.

Declarations

Conflict of interest The authors declare that they have no known competing financial interests or personal relationships that could have appeared to influence the work reported in this paper.

Acknowledgments

The work described in this study was supported by the National Natural Science Foundation of China [Grant Nos. 52175387 and 52075104]. We sincerely thank Xinlang Zuo for their support with the SEM and EDS (the China Electronic Product Reliability and Environmental Testing Research Institute).

References

1. Masuzawa, T. (2000). State of the art of micromachining. *CIRP Annals-Manufacturing Technology*, 49, 473-488.

2. Hasan, M., Zhao, J., & Jiang, Z. (2017). A review of modern advancements in micro drilling techniques. *Journal of Manufacturing Processes*, 29, 343-375.

3. Chu, W. S., Kim, C. S., Lee, H. T., Choi, J. O., Park, J. I., Song, J. H., Jang, K. H., & Ahn, S. H. (2014). Hybrid manufacturing in micro/nano scale: A Review. *International Journal of Precision Engineering and Manufacturing-Green Technology*, 1(1), 75-92.

4. Nasrollahi, V., Penchev, P., Batal, A., Le, H., Dimov, S. & Kim, K. (2020). Laser drilling with a top-hat beam of micro-scale high aspect ratio holes in silicon nitride. *Journal of Materials Processing Technology*, 281, 116636.

5. Heo, J., Min, H., & Lee, M. (2015). Laser Micromachining of Permalloy for Fine Metal Mask. *International Journal of Precision Engineering and Manufacturing-Green Technology*, 2(3), 225-230.

6. Chen, Xiaolei., Zhu, Jiajun., Xu, Zhongzheng., & Su, Guokang. (2021). Modeling and experimental research on the evolution process of micro through-slit array generated with masked jet electrochemical machining. *Journal of Materials Processing Technology*, 298, 117304.

7. Chung, D. K., & Chu, C. N. (2015). Effect of Inductance in Micro EDM Using High Frequency Bipolar Pulse Generator. *International Journal of Precision Engineering and Manufacturing-Green Technology*, 2(3), 299-303.

8. Islam, M. M., Li, C. P., & Ko, T. J. (2017). Dry electrical discharge machining for deburring drilled holes in CFRP composite. *International Journal of Precision Engineering and Manufacturing-Green Technology*, 4(2), 194-154.

9. Zia, M. K., Pervaiz, S., Anwar, S., & Samad, W. A. (2019). Reviewing Sustainability Interpretation of Electrical Discharge Machining Process using Triple Bottom Line Approach. *International Journal of Precision Engineering and Manufacturing-Green Technology*, 6(5), 931-945.

10. Tsai, Y. Y. (2004). An index to evaluate the wear resistance of the electrode in micro-EDM. *Journal of Materials Processing Technology*, 149(1-3), 304-309.

11. Li, G., Natsu, W., & Yu, Z. (2019). Study on quantitative estimation of bubble behavior in micro hole drilling with EDM. *International Journal of Machine Tools & Manufacture*, 146, 103437.

12. Ferraris, E., Castiglioni, V., Ceyssens, F., Annoni, M., Lauwers, B., & Reynaerts, D. (2013). EDM drilling of ultra-high aspect ratio micro holes with insulated tools. *CIRP Annals-Manufacturing Technology*, 62(1), 191-194.

518 13. Wang, Y., F, Zhao., & Jin, W. (2009). Wear-resist Electrodes for Micro-EDM. *Chinese Journal of*
519 *Aeronautics*, 22(3), 339-342.
520 14. Kumar, R., & Singh, I. (2019). A modified electrode design for improving process performance of
521 electric discharge drilling. *Journal of Materials Processing Technology*, 264, 211-219.
522 15. D'Urso, G., Longo, M., Maccarini, G., & Ravasio, C. (2011). Electrical discharge machining of
523 micro holes on titanium sheets. *Proceedings of the ASME Design Engineering Technical*
524 *Conference*, 417-424.
525 16. Jahan, M. P., Wong, Y. S., & Rahman, M. (2009). A study on the quality micro-hole machining of
526 tungsten carbide by micro-EDM process using transistor and RC-type pulse generator. *Journal of*
527 *Materials Processing Technology*, 209(4), 1706-1716.
528 17. Yan, Mu-Tian., & Liu Yi-Ting. (2009). Design, analysis and experimental study of a
529 high-frequency power supply for finish cut of wire-EDM. *International Journal of Machine*
530 *Tools & Manufacture*, 49,793-796.
531 18. Yang, Jiao., Yang, Fei., Hua, Han., Cao, Yong., Li, Chunhui., & Fang, Bin. (2018). A Bipolar
532 Pulse Power Generator for Micro-EDM. *Procedia CIRP*, 68, 620-624.
533 19. Huan, L., Jicheng, B., Yan, C., Guozheng, Z., & Shaojie, H. (2020). Micro-electrode wear and
534 compensation to ensure the dimensional consistency accuracy of micro-hole array in micro-EDM
535 drilling. *International Journal of Advanced Manufacturing Technology*, 111(9-10), 2653-2665.
536 20. Mustafa, Ay., Ulaş, Çaydaş., & Ahmet, Hasçalık. (2013). Optimization of micro-EDM drilling of
537 inconel 718 superalloy. *International Journal of Advanced Manufacturing Technology*, 66(5-8),
538 1015-1023.
539 21. Pei, Jingyu., Zhang, Lenan., Du, Jianyi., Zhuang, Xiaoshun., Zhou, Zhaowei., Wu, Shunkun., &

Zhu, Yetian. (2017). A Model of Tool Wear in Electrical Discharge Machining Process Based on Electromagnetic Theory. *International Journal of Machine Tools & Manufacture*, 117, 31-41.

22. Jeong, Y.H., & Min, B.K. (2007). Geometry prediction of EDM-drilled holes and tool electrode shapes of micro-EDM process using simulation. *International Journal of Machine Tools & Manufacture*, 47(12-13), 1817-1826.

23. Aligiri, E., Yeo, S.H., & Tan, P.C. (2010). A new tool wear compensation method based on real-time estimation of material removal volume in micro-EDM. *Journal of Materials Processing Technology*, 210(15), 2292-2303.

24. Malayath, G., Katta, S., Sidpara, A., & Deb, S. (2019). Length-wise tool wear compensation for micro electric discharge drilling of blind holes. Measurement, 134, 888-896.

25. Pham, D.T., Ivanov, A., Bigot, S., Popov, K., & Dimov, S. (2007). An investigation of tube and rod electrode wear in micro EDM drilling. *International Journal of Advanced Manufacturing Technology*, 33(1-2), 103-109.

26. Mitsui, K., & Mahardika, M. (2008). A new method for monitoring micro-electric discharge machining process. *International Journal of Machine Tools & Manufacture*, 48(3-4), 446-458.

27. Ekmekci, B., Sayar, A., O¨pöz, T.T., & Erden, A. (2009). Geometry and surface damage in micro electrical discharge machining of micro-holes. *Journal of Micromechanics & Microengineering*,19, 105030.

28. Schacht, B., Kruth, J., Lauwers, B., & Vanherck, P. (2004). The skin-effect in ferromagnetic electrodes for wire-EDM. *International Journal of Advanced Manufacturing Technology*, 23(11-12), 794-799.

29. Li, X., Wang, Y., Liu, Y., & Zhao, F. (2019). Research on Shape Changes in Cylinder Electrodes

Incident to Micro-EDM. *Advances in Materials Science and Engineering*, 2019(4), 1-11.

30. Ekmekci, Bülent., & Sayar, A. (2013). Debris and consequences in micro electric discharge machining of micro-holes. *International Journal of Machine Tools & Manufacture*, 65, 58-67.

31. Ichikawa, Tomohiko., & Natsu, Wataru. (2013). Investigation of Machining Characteristics of Micro-EDM with Ultrasonically Vibrated Machining Fluid under Ultra-small Discharge Energy. *International Journal of Electrical Machining*,18, 1-7.

32. Ikeno, J., Tani, Y., & Sato, H. (1990). Nanometer Grinding Using Ultrafine Abrasive Pellets - Manufacture of Pellets Applying Electrophoretic Deposition. *CIRP Annals-Manufacturing Technology*, 39(1), 341-344.

33. Mangelsdorf, C.S., & White, L.R. (1992). Electrophoretic Mobility of a Spherical Colloidal Particle in an Oscillating Electric Field. *Journal of the Chemical Society Faraday Transactions*, 88(24), 3567-3581.

34. Einstein, A. (1926). Die Ursache der Manderbildung der Flulufe und des sogenannten Baerschen Gesetze. *Naturwissenschaften*, 14(11), 223-224.

Biography

Zhixiang Zou is a Ph.D. candidate in school of electromechanical engineering, Guangdong University of Technology. His research interests include non-traditional machining and precision engineering.

Xiaoyu Zhang is a Ph.D. candidate in in College of Mechanical and Electrical Engineering at Central South University. Her research interests include polymer micro-nano manufacturing and precision molding.

Kangcheung Chan is Head of the Department of Industrial and Systems Engineering of The Hong Kong Polytechnic University. He received his Ph.D. in the Hong Kong Polytechnic University. Currently, he is the undergraduate programmes director of the Dept., laboratory-in-charge of Materials Engineering Laboratory, and the programme leader of the Bachelor of Engineering programme. His research areas include processing and properties of advanced materials, electrodeposition of metals and oxides.

Taiman Yue is a Professor in department of industrial and systems engineering of the Hong Kong Polytechnic University. He received his Ph.D. in department of engineering materials of University of Southampton UK. His research focuses on advanced manufacturing technology and composite materials.

Zhongning Guo is a Professor in school of electromechanical engineering at Guangdong University of Technology. He received his Ph.D. in industrial and systems engineering department from the Hong Kong Polytechnic University. His research focuses on micro machining and non-traditional machining.

Can Weng is a Professor in College of Mechanical and Electrical Engineering at Central South University. She received her Ph.D. in Industrial and Systems Engineering department from the Hong Kong Polytechnic University. Her research focuses on micro-nano manufacturing and precision molding.

Jiangwen Liu received his Ph.D. in industrial and systems engineering department from the Hong Kong Polytechnic University in 2010. He joined Guangdong University of Technology as an associate professor of mechanical engineering in 2016. His current research focuses on non-traditional machining.